Comparison of satellite-based cloud-top height and wind from MISR, ATSR2 and Meteosat-6 Rapid Scans

Presented Paper to EUMETSAT Data Users' Conference, Antalya, 1 – 5 October 2001

COMPARISON OF SATELLITE-BASED CLOUD-TOP HEIGHT AND WIND FROM MISR, ATSR2 AND METEOSAT-6 RAPID SCANS

Gabriela SEIZ [1, 2], Manos BALTSAVIAS [1]

[1] Institute of Geodesy and Photogrammetry, ETHZ, CH-8093 Zuerich
[2] MeteoSwiss, Kraehbuehlstrasse 58, CH-8044 Zuerich

ABSTRACT

This paper describes the comparison of MISR cloud-top height (CTH) and wind (CTW) results with the CTH and CTW derived from coincident ATSR2 and Meteosat-6 10-min Rapid Scans in August 2000. Both the operational MISR cloud product (level 2TC) from NASA-JPL and our own CTH/CTW-results (starting from level 1B2 data) are used for the comparison.

The results from the case study in August 2000 show in general a good agreement between the derived CTH and CTW from the three satellite systems. The advantage of MISR to simultaneously determine CTH and CTW, using at least three non-symmetric cameras, is important as the large wind induced height errors in stereo CTH retrievals from slightly asynchronous satellite stereo pairs (e.g. ATSR2) have to be corrected otherwise with additional CTW information, e.g. from the Meteosat-6 Rapid Scans. The matching statistics of the various camera combinations indicate however that the correspondences between non-adjacent cameras (e.g. AN and DF as used for the motion retrieval of the operational product) can be quite tricky because the cloud objects have changed their shapes or even disappeared in the delay between the two views. While the matching success rate is about 95% for adjacent cameras, it decreases towards about 78% between the nadir and the outermost camera (DF).

Finally, as a preliminary ground validation, a radiosounding from Western Switzerland was used. Both the CTH estimation and the wind measurements show a good correspondence with the satellite-based CTH and CTW results. Despite of the good agreement within this case study, it has to be noted that conventional wind data do not necessarily correspond to the cloud motion, in particular over land and in mountainous terrain. The Meteosat-6 Rapid Scan Service, which is operational since September 2001, is therefore a perfect opportunity to study the degree of correspondence between wind fields and cloud motion fields, which is important for the assimilation of satellite-based cloud products into regional NWP models.

1. INTRODUCTION

Stereoscopy of clouds has a long tradition in meteorology (Hasler, 1981). From satellites, both geostationary and polar-orbiting sensors can be used, as described in Fujita (1982). Stereo measurements have the advantage that they depend only on basic geometric relationships of observations of cloud features from at least two different viewing angles, while other cloud top height estimation methods are dependent on the knowledge of additional cloud/atmosphere parameters like cloud emissivity, ambient temperature or lapse rate.

In contrast to ground-based multiple camera systems, stereo image pairs from polar-orbiting satellites are never perfectly synchronous. There is a time delay of some seconds between the image acquisition from the different viewing angles. While this is no problem for digital terrain model (DTM) generation of non-moving objects (land surface, etc.), the height error for stereo cloud-top height retrievals can be quite large depending on the along-track cloud motion. In a previous paper (Seiz and Baltsavias, 2000a), we have shown the successful use of the Meteosat-6 5-min Rapid Scans during the Mesoscale Alpine Programme (MAP) to correct these wind errors for ERS2-ATSR2 cloud-top heights.

Campbell (1998), shows the possibilities and limits of direct asynchronous stereo height analysis for various satellite constellations.

This study is part of the EU-project CLOUDMAP2 which has a key objective to compare different retrieval methods of cloud properties. Our stereo retrieval method can help in the validation work of the two macroscopic parameters 'cloud-top height' (CTH) and 'cloud-top wind' (CTW). Further validation is planned with various ground-based remote sensing instruments: radiosoundings, ceilometers and a newly developed stereo camera system (Seiz and Baltsavias, 2000b).

2. ATSR2 CTH (WIND-CORRECTED)

The ATSR2 instrument is part of the ERS-2 satellite system which was launched in April 1995. The successor sensor, AATSR, will be part of Envisat which is currently scheduled for December 2001. ERS-2 is in a near-circular, sun-synchronous orbit at a mean height of 780km, an inclination of 98.5 and a sub-satellite velocity of 6.7 km/s. The spacecraft is positioned to operate with a descending equator crossing of around 10:30 local solar time and of a ascending equator crossing of 22:30 local solar time. The repeat cycle is about 3 days.

First, the ATSR2 views the surface along the direction of the orbit track at an incidence angle of 55° as it flies toward the scene. Then, some 120s later, ATSR2 records a second observation of the scene at an angle close to the nadir (Mutlow, 1999). ATSR2's field of view comprises two 500 km-wide curved swaths, with 555 pixels across the nadir swath and 371 pixels across the forward swath. The pixel size is 1x1 km at the center of the nadir scan and 1.5 x 2 km at the center of the forward scan. The sensor records in 7 spectral channels: 0.55ìm, 0.67 ìm, 0.87 ìm, 1.6 ìm, 3.7 ìm, 10.8 ìm, 12.0 ìm, which is comparable to the channels of the new SEVIRI instrument on MSG. The geolocation for the rectified (GBT) products proceeds by mapping the acquired pixels onto a 512x512 grid with 1km pixel size whose axes are the ERS-2 satellite ground-track and great circles orthogonal to the ground-track.

2.1 Cloud-top height retrieval

The ATSR2 GBT data were reduced to 8-bit and linearly stretched between the minimum and maximum value, cutting 0.5% on both sides of the histogram (excluding the pixels assigned with an error code). As no a priori values of the cloud heights are given to the matching algorithm, a hierarchical matching procedure with 3 pyramid levels is applied so that the maximum possible parallax at the highest level is only 1-2 pixels. Every pyramid level is enhanced and radiometrically equalized with a Wallis filter (Wallis, 1976). Points with good texture are selected with an interest operator (Förstner and Gülch, 1987) in the first pyramid level because it is likely that the same points are well detectable also in the other levels. The matching was done with the Multi-Photo Geometrically Constrained Matching Software package developed at our institute (Baltsavias, 1991), which is based on Least-Squares-Matching (LSM) (Grün, 1985). The matching solutions are quality-controlled with absolute and relative tests on the matching statistics. The resulting y-parallaxes are converted into cloud heights after (Prata and Turner, 1997), considering that the zenith angles have to be projected on the along-track plane.

The height values of the successfully matched points are finally interpolated to the 512x512 grid. Three cloud tests are applied on the ATSR2 data to separate cloud, land and mixed pixels: 1) 0.87ìm/11.0ìm-ratio test, 2) 11.0ìm-3.7ìm difference test and 3) 3.7ìm-12.0ìm difference test. If a pixel fulfilled all tests, it was classified as cloudy; if none of the tests were fulfilled, the pixel was marked as land; all other pixels were classified as mixed. Only the cloudy pixels were then selected for the further investigations. Statistics of the results of the mixed and land pixels showed that many blunders could not be detected by the quality control within these areas. This is caused by multiple solutions within the land surface at this spatial resolution and by the problem that the matching result – especially at higher pyramid levels – is strongly affected by the near cloud borders.

2.2 Across-track wind retrieval and along-track wind error

The forward and nadir ATSR2 images were acquired with a mean time delay of 120 seconds so that significant cloud motion is observable between the two scans. For the across-track wind retrieval and along-track wind correction, described in Section 3.2, the exact time difference between the corresponding pixels in the forward and the nadir scan is calculated from the along-track distance on the ground and the satellite velocity after (Lorenz, 1985).

3. METEOSAT-6 CTW

Following the success of the 5min Rapid Scanning support provided to the Mesoscale Alpine Programme (MAP) in Autumn 1999, new 10min Rapid Scans were started by EUMETSAT in August 2000. These trials had normally a duration of 48 to 72 hours a week. Since September 2001, an operational 10min Rapid Scanning Service (RSS) is

maintained. For the rapid scans, the in-orbit stand-by Meteosat-6 instrument, positioned at 9 W, is used. The limited scan consists of 5000 x 1666 pixels (or 2500 x 833 for IR/WV), starts at line 2948 (or line 1474 for IR/WV) of the operational Meteosat-7 scan and covers an area approximately from 10 to 70º N (Figure 1). (EUMETSAT, 2001)

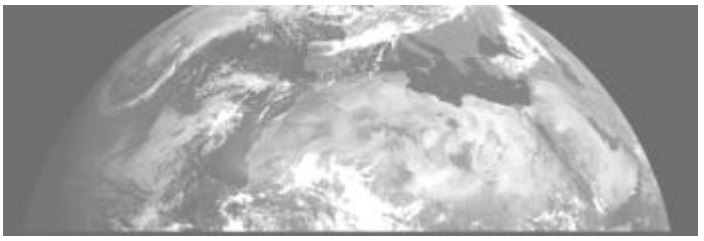

Figure 1. Meteosat-6 Scan Area in August 2000.

3.1 Tracking

Before tracking, the images were enhanced with a Wallis filter for contrast enhancement. The corresponding points in the image sequence were then determined with our least-squares matching (LSM) algorithm. Because of the larger disparities (up to about 10 pixels) compared with the 5min MAP Rapid Scans, two pyramid levels (original + 1st pyramid level) were used in the matching. As the features – even clouds – are very self-similar within these 10 minutes, the tracking of cloud points is much easier compared to tracking of the operational 30min Meteosat-7 series where it can be difficult to select good cloud tracers (Schmetz et al., 1993).

3.2 Wind correction for ATSR2

The Meteosat-6 motion vectors were resampled to the 512 x 512 ATSR2 grid, and the across-track and along-track components calculated. With the time difference between nadir and forward acquisition (pixel-dependent), the along-track components are converted into the CTH correction amounts. North winds lead to an underestimation of the heights so that the along-track wind component has to be added to the y-parallax while southerly winds result in too high cloud-top heights. The across-track component can be used as a comparison to the ATSR2 x-disparity field (scaled with height factor h); large discrepancies would indicate matching, tracking or geolocation errors.

4. MISR CTH AND CTW

The Multi-angle Imaging SpectroRadiometer (MISR) was launched aboard the EOS AM-1 Terra spacecraft in December 1999. The orbit is sun-synchronous at a mean height of 705km, with an inclination of 98.5 and anequatorial crossing time at about 10:30 a.m. The repeat cycle is 16 days.

The MISR instrument consists of nine pushbroom cameras at different viewing angles: -70.5º (named DA), -60.0º (CA), -45.6º (BA), -26.1º (AA), 0.0º (AN), 26.1º (AF), 45.6º (BF), 60.0º (CF), and 70.5º (DF). The time delay between adjacent camera views is 45-60 seconds which results in a total delay between the DA and DF image of about 7 minutes. Each camera uses four Charge-Coupled Device (CCD) line arrays in a single focal plane. The line arrays consist of 1504 photoactive pixels plus a set of light-shielded pixels per array, each 21 mm x 18 mm. Each line array is filtered to provide one of four MISR spectral bands. The spectral band shapes are nominally gaussian, and centered at 446 (blue), 558 (green), 672 (red), and 866 nm (NIR). The data of the red band from all nine cameras and of the blue, green and NIR bands of the AN camera are saved in high-resolution, with a pixel size of 275 x 275 m; the data of the blue, green and NIR bands of the remaining eight cameras are stored in low-resolution , with a pixel size of 1.1 x 1.1 km.

The operational data products from NASA are described in Lewicki et al. (1999). The two products used for this study are the L1B2 Ellipsoid data (geolocated product) and the L2TC data (top-of-the-atmosphere/ cloud product).

4.1 Own algorithms

The MISR L1B2 Ellipsoid data were reduced to 8-bit and linearly stretched between the minimum and maximum value. As no a priori values of the cloud heights are given to the matching algorithm, a hierarchical matching procedure with 5 pyramid levels is applied so that the maximum possible parallax at the highest level is only a few pixels. Every pyramid level is enhanced and radiometrically equalized with a Wallis filter. Points with good texture are selected with the Foerstner interest operator in the third pyramid level. The matching was done as for the ATSR2 images with the Multi-Photo Geometrically Constrained Matching Software package developed at our institute. Especially between non-adjacent cameras, the matching is more difficult and will need some adaptations of the algorithm to deal with shape changes and appearance/disappearance of cloud features (Figure 2 and Table 1).

The resulting x- and y-parallaxes from three non-symmetric views (e.g. AN-AA-CF) are converted into CTH, along-track and across-track wind components with the linear equations described in Diner et al. (1999). In the equations, the zenith angles from the Ancillary Geometric Product and the coefficients provided in the L1B2 metadata to calculate the exact acquisition time of each pixel are used.

	AN-AA	AN-AF	AN-BF	AN-CF	AN-DF
# points	52877	52214	48512	42653	35730
# matched points	49840	49329	42751	35241	27941
Success rate [%]	94.3	94.5	88.1	82.6	78.2
Iterations/ point	5.7	5.7	7.8	9.1	9.8

Table 1. Success rate of the LSM algorithm with different camera combinations on the original level.

4.2 Operational NASA-JPL cloud products (Level 2TC)

Stereo CTH on a 1.1 x 1.1 km grid and CTW on a 70.4 x 70.4 km grid are provided within the operational MISR processing chain as part of the level 2TC product. The algorithms applied for the CTH and CTW retrieval are described in Diner et al. (1999). Important to note is that no subpixel matching algorithm is used and that the CTH and CTW for the high-resolution 1.1x1.1km CTH product are not retrieved simultaneously, but in two steps.

5. RESULTS

All the above described methods were applied to the dataset in August 2000 with coincident images of MISR, ATSR2 and Meteosat-6 (within 15 minutes). Table 2 shows the exact acquisition periods of the three satellite systems.

Sensor	Start	End	Approximate time at 47º N (SN-scanning of Meteosat-6)	Frequency
MISR (blocks 49-55)	DF: 10:49:32 AN: 10:52:58	DF: 10:52:02 AN: 10:55:28		16 days
ATSR2	forward: 10:45:02 nadir: 10:47:02	forward: 10:46:18 nadir: 10:48:18		About 3 days
Meteosat-6	10:30/ 10:40/ ...	10:38:20/ 10:48:20/ ...	10:37:21/ 10:47:21/ ...	10 min

Table 2. Acquisition times of the different sensors for case study in August 2000.

In the cloud-top height map from ATSR2 (Fig. 4), two cloud systems can be distinguished, one at the right side with heights of 6000 m and higher, and many smaller cloud objects towards the upper left at lower heights (between 2000 and 6000 meters). The cloud systems can also be distinguished in the motion field, extracted from the Meteosat-6 Rapid Scans, where the lower layers move much slower and more towards the east in contrast to the fast moving high cloud layer, moving towards north-east.

The wind correction for the ATSR2 cloud-top heights which as derived from the Meteosat-6 wind field, is summarized in Table 3. The along-track wind component in this case is quite substantial and leads to an overestimation of the CTH of up to 5.3 km for the cloud system over Western Switzerland. Figure 3 shows the distribution of the CTH correction due to the along-track motion and in Figure 4, the resulting wind-corrected ATSR2 CTH map is drawn.

	Mean	Min	Max
x wind component [m/s]	12.3 ± 5.1	-1.9	27.8
y wind component [m/s]	12.5 ± 10.0	-17.3	42.6
x-shift [m]	1518.0 ± 628.5	-189.6	3732.4
y-shift [m]	1538.9 ± 1219.2	-1818.5	5291.3

Table 3. Statistics of the Meteosat-6 cloud motion field within the ATSR2 field of view.

The MISR L2TC StereoHeight product (Figure 6) displays similar CTH structures as the ATSR2 CTH map; only some sort of blocking within the results (especially in the lower part of the map) is clearly visible which obviously comes from large discontinuities in the sparse CTW field. As comparison, the along-track disparity map is shown in Figure 5 where the CTH are smooth and the blocking is not present at all which proves that the blocking is introduced in the second step of wind correction. The 70.4 x 70.4 km CTW grid is probably too sparse, especially over land and mountainous terrain. It is very likely that the wind field is not homogenous within such a large grid cell, and as consequence, the CTH field is not accurately corrected.

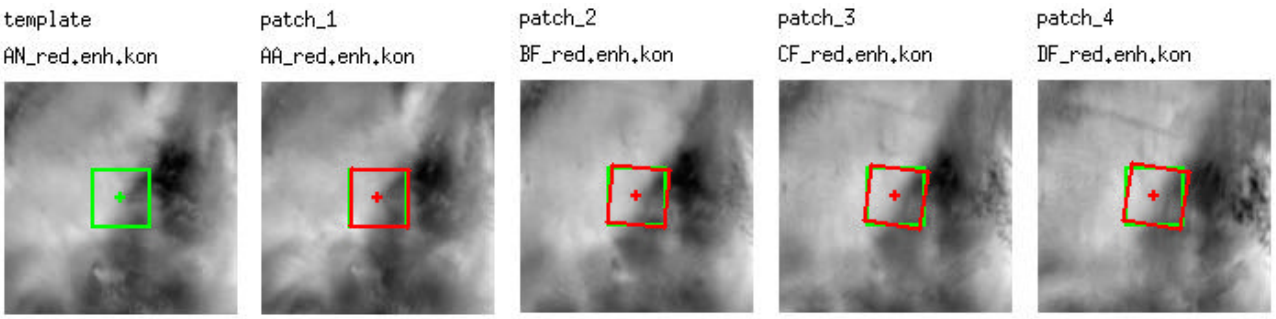

Figure 2. Matching difficulties between the AN, AA, BF, CF and DF camera views.

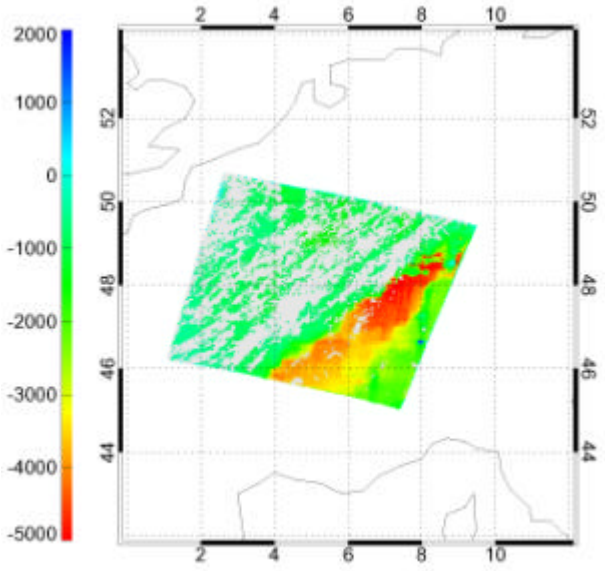

Figure 3. ATSR2 CTH correction amounts (in meters), as derived from Meteosat-6 (grey: cloud mask).

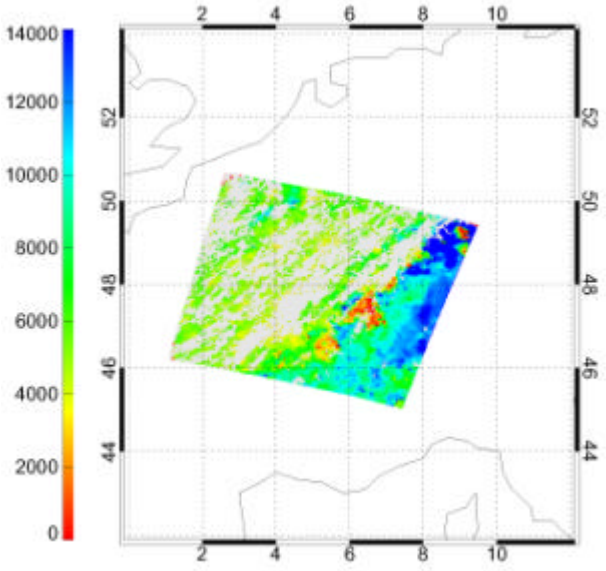

Figure 4. ATSR2 CTH, wind-corrected (in meters, grey: cloud mask).

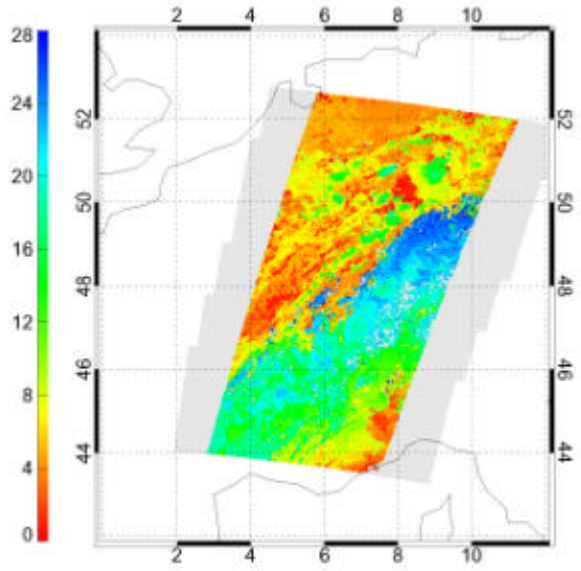

Figure 5. MISR L2TC along-track disparity (in pixels, grey: no retrieval).

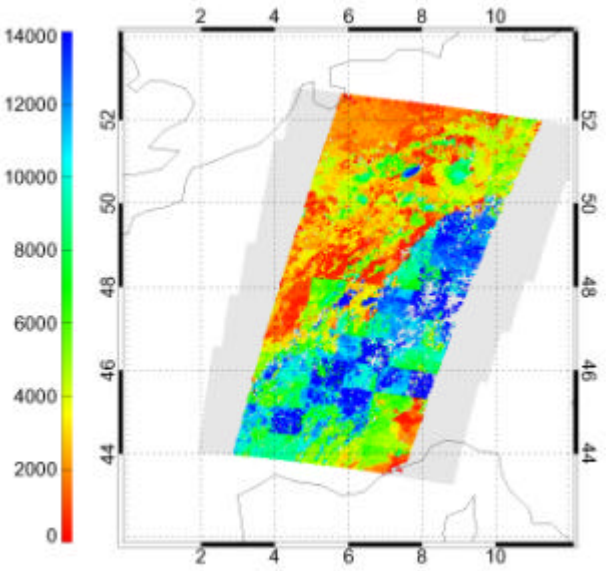

Figure 6. MISR L2TC StereoHeight (in meters, grey: no retrieval).

6. COMPARISON WITH GROUND-BASED DATA

6.1 Radiosondes

Figure 7 shows the radiosounding launched at Payerne (CH, 46.82º N, 6.95º E) at 12:00 UTC. According to the method described in (Chernykh and Eskridge, 1996), the top of the highest cloud layer can be identified at about 6700-7000 m above sea level which corresponds to the heights of the ATSR2 and MISR CTH maps (Figure 4 and 6).

The wind vectors from the 06:00 and the above mentioned 12:00 sounding are in good agreement with the satellite-based CTW vectors from Meteosat-6 (Table 4).

Payerne, 46.82ºN, 6.95ºE	Sounding 06:00	Sounding 12:00	M-6 CTW
Speed [m/s]	30 - 35	25 - 30	39.6
Direction [º]	240	225	223
Speed along-track [m/s]	23.0	24.9	33.6
Speed across-track [m/s]	26.4	16.8	21.0

Table 4. Comparison of wind measurements from the operational MeteoSwiss soundings with the Meteosat-6 Rapid Scans CTW.

However, in general, such comparison of cloud motion fields and wind fields are problematic, especially over land and with orography. Therefore, any comparison with other wind measurements (wind profilers, radiosonde winds, NWP model wind fields) is limited and should be only carried out carefully.

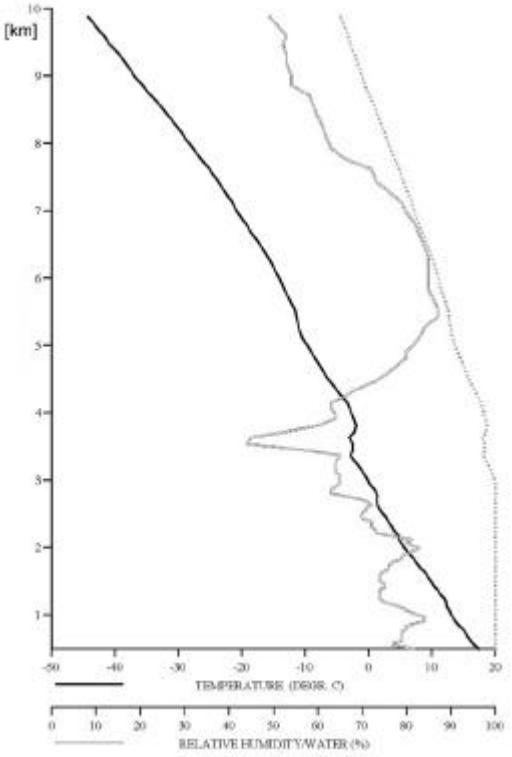

Figure 7. Radiosounding, launched at Payerne at 12.00 UTC (Source: Aerological station, MeteoSwiss).

7. CONCLUSIONS

The preliminary results from the case study in August 2000 show the high value of comparison possibilities between the CTH and CTW products from different satellite sensors and various retrieval methods. For ATSR2 Stereo CTH, it has proven to be absolutely necessary to correct them with CTW data from another source. Over land and mountainous regions, the cloud motion is most accurately derived from simultaneous images of a geostationary satellite. In Europe, the operational Meteosat-6 10min Rapid Scans (since September 2001) are perfectly suited for this objective.

The accurate determination of satellite cloud-top heights depends strongly on a precise sensor model (or regridding algorithm) and on a robust matching technique. Our hierarchical matching approach with subpixel accuracy showed to be usable for the task of cloud matching. A special effort will be taken to improve the matching process between images with longer time delays where the shape of the cloud features has changed and/or some features have even appeared or disappeared from one view to the other. As any regridding errors can additionally influence the x- and y-parallaxes, exact knowledge about the rectification process is needed. For MISR images, the geolocation accuracy will be studied in the near future by applying an own sensor model, while the accuracy of the ATSR2 regridding will not be evaluated further.

ACKNOWLEDGEMENTS

The EOS-Terra MISR data (level 1B2 and level 2TC) were obtained from the NASA Langley Research Center Atmospheric Sciences Data Center, the Meteosat-6 and Meteosat-7 data from the EUMETSAT MARF Archive Facility and the ATSR2 data were received via the ESA ATSR2 NRT service. We thank Catherine Moroney, University of Arizona, for the reprocessing of the MISR dataset and for valuable input in the understanding of the L2TC products, and Chris Hansen, EUMETSAT, for answers about the Meteosat-6 data. This work is funded by the Bundesamt für Bildung und Wissenschaft (BBW) within the EU-project CLOUDMAP2 (BBW Nr. 00.0355-1).

REFERENCES

Baltsavias, E.P., 1991. Multiphoto Geometrically Constrained Matching. Ph. D. dissertation, Institute of Geodesy and Photogrammetry, ETH Zurich, Mitteilungen No. 49, 221 p.

Campbell, G.G., 1998. http://www.cira.colostate.edu/GeoSci/windZ/windz.html (accessed September 27, 2001).

Chernykh, I.V., Eskridge, R.E., 1996. Determination of cloud amount and level from radiosonde soundings. J. Appl. Met., **35**, 8, pp. 1362-1369.

Diner, D. et al., 1999. MISR Level 2 Cloud Detection and Classification. MISR Algorithm Theoretical Basis Documents, ATBD-MISR-07. NASA JPL. http://eospso.gsfc.nasa.gov/atbd/misrtables.html (accessed September 27, 2001).

EUMETSAT, 2001. http://www.eumetsat.de/en/index.html?area=left7.html&body=/en/dps/dissemination/rss.html (accessed September 27, 2001).

Förstner, W., Gülch, E., 1987. A fast operator for detection and precise location of distinct points, corners, and centers of circular features. Proc. ISPRS Intercommission Conf. on Fast Processing of Photogrammetric Data, Interlaken, Switzerland, 2-4 June, pp. 281-305.

Fujita, T.T., 1982. Principle of stereoscopic height computations and their applications to stratospheric cirrus over severe thunderstorms. J. Met. Soc. Japan, **60**, 1, pp. 355-368.

Grün, A., 1985. Adaptive least squares correlation: a powerful image matching technique. S. Afr. J. of Photogrammetry, Remote Sensing and Cartography, **14**, 3, pp. 175-187.

Hasler, F., 1981. Stereographic observations from geosynchronous satellites: an important new tool for the atmospheric sciences. Bull. Am. Met. Soc., **62**, 2, pp. 194-212.

Lewicki, S. et al., 1999. MISR Data Products Specifications. NASA JPL. http://eosweb.larc.nasa.gov/PRODOCS/misr/readme/dps_ne_icd.pdf (accessed September 27, 2001).

Lorenz, D., 1985. On the feasibility of cloud stereoscopy and wind determination with the along-track scanning radiometer. Int. J. Rem. Sens., **6** , 8, pp. 1445-1461.

Mutlow, Ch., 1999. ATSR-1/2 User Guide, Issue 1.0. Rutherford Appleton Laboratory.

Prata, A.J., Turner, P.J., 1997. Cloud-top height determination using ATSR data. Rem. Sens. Env., **59**, 1, pp. 1-13.

Schmetz, J., Holmlund, K., Hoffman, J., Strauss, B., Mason, B., Gaertner, V., Koch, A., Van de Berg, L., 1993. Operational cloud-motion winds from Meteosat infrared images. J. Appl. Met., **32**, 7, pp. 1206-1225.

Seiz, G., Baltsavias, E.P., 2000a. Satellite- and ground-based stereo analysis of clouds during MAP. EUMETSAT Conference Proceedings, Bologna, pp. 805-812.

Seiz, G., Baltsavias, E.P., 2000b. Cloud mapping using ground-based imagers. In: International Archives of Photogrammetry and Remote Sensing (IAPRS), **33**, Part B7/4, pp. 1349-1356.

Wallis, R., 1976. An approach to the space variant restoration and enhancement of images. Proc. of Symp. on Current Mathematical Problems in Image Science, Naval Postgraduate School, Monterey CA, USA, November.